To appear in ApJL
Preprint typeset using LaTeX style emulateapj v. 08/22/09

ALMA 690 GHZ OBSERVATIONS OF IRAS 16293-2422B: INFALL IN A HIGHLY OPTICALLY-THICK DISK

Luis A. Zapata[1], Laurent Loinard[1,2], Luis F. Rodríguez[1,3], Vicente Hernández[1],
Satoko Takahashi[4], Alfonso Trejo[4], and Bérengère Parise[2]

To appear in ApJL

ABSTRACT

We present sensitive, high angular resolution ($\sim$ 0.2 arcsec) submillimeter continuum and line observations of IRAS 16293-2422B made with the Atacama Large Millimeter/Submillimeter Array (ALMA). The 0.45 mm continuum observations reveal a single and very compact source associated with IRAS 16293-2422B. This submillimeter source has a deconvolved angular size of about 400 *milli-arcseconds* (50 AU), and does not show any inner structure inside of this diameter. The $H^{13}CN$, $HC^{15}N$, and CH_3OH line emission regions are about twice as large as the continuum emission and reveal a pronounced inner depression or "hole" with a size comparable to that estimated for the submillimeter continuum. We suggest that the presence of this inner depression and the fact that we do not see inner structure (or a flat structure) in the continuum is produced by very optically thick dust located in the innermost parts of IRAS 16293-2422B. All three lines also show pronounced inverse P-Cygni profiles with infall and dispersion velocities larger than those recently reported from observations at lower frequencies, suggesting that we are detecting faster, and more turbulent gas located closer to the central object. Finally, we report a small east-west velocity gradient in IRAS 16293-2422B that suggests that its disk plane is likely located very close to the plane of the sky.

Subject headings: stars: pre-main sequence – ISM: jets and outflows – ISM: individual: (IRAS 16293−2422) – techniques: spectroscopic

1. INTRODUCTION

Located at a distance of 120 pc (Loinard et al. 2008) in the ρ Ophiuchi star forming region, IRAS 16293−2422B, is a well-studied low-mass very young star. Together with its close-by companion separated by only 600 AU (IRAS 16293−2422A), the entire region (IRAS 16293−2422) has a bolometric luminosity of 25 $L_\odot$, and is embedded in a 2 $M_\odot$ envelope of size $\sim$ 2000 AU (Correia et al. 2004). Both sources show a very rich and complex chemistry, with hot-core-like (hot-corino) properties at scales of $\sim$ 100 AU and temperatures of about 100 K (Ceccarelli et al. 1998; Cazaux et al. 2003; Bottinelli et al. 2004; Chandler et al. 2005; Caux et al. 2011).

Sensitive and high angular resolution observations at 7 mm revealed a compact, possibly isolated disk associated with IRAS 16293−2422B with a Gaussian half-power radius of only 8 AU (Rodríguez et al. 2005). However, the search for an outflow associated with this source has been a hard task. Jørgensen et al. (2011) using submillimeter (SMA) observations of IRAS 16293−2422 with a relatively high angular resolution resolved the A and B components, and did not find any strong indications for high velocity gas toward B. Yeh et al. (2008) reported the detection of a compact blue-shifted CO structure to the south-east of source B, and mentioned that it might correspond to a compact outflow ejected from source B. Loinard et al. (2012) using ALMA observations revealed indeed that the source B is driving a south-east blueshifted compact outflow. However, the flow has peculiar properties: it is highly asymmetric, bubble-like, fairly slow (10 km s^{-1}), and lacking of a jet-like feature along its symmetry axis. In addition, its dynamical age is only about 200 years.

One of the first evidences of the detection of infall motions associated with IRAS 16293−2422B came from Chandler et al. (2005) using Submillimeter Array (SMA) observations at 300 GHz. More recently, Pineda et al. (2012) using ALMA Science Verification observations with high-spectral resolution studied the gas kinematics with detail in IRAS 16293−2422B at 220 GHz, and reported clear inverse P-Cygni profiles toward this source in their three brightest lines and derived from a simple two-layer model an infall rate of 4.5×10^{-5} $M_\odot$ yr^{-1}, which is a typical value for low-mass protostars.

In this *Letter*, we report ∼0.2 arcsec resolution 690 GHz observations obtained with the Atacama Large Millimeter/Submillimeter Array (ALMA) from the object IRAS 16293-2422B. The continuum observations reveal a very compact source with a deconvolved angular size of about 400 *milli-arcseconds* or a spatial size of about 50 AU, while the line emission shows a clear pronounced inner depression or "hole" in the middle of IRAS 16293−2422B. All the three lines mapped in this study show pronounced inverse P-Cygni profiles.

2. OBSERVATIONS

The observations were made with fifteen antennas of ALMA on April 2012, during the ALMA science verification data program. The array at that point only included antennas with diameters of 12 meters. The 105 independent baselines ranged in projected length from 26 to 403 m. The observations were made in mosaicing mode using a half-power point spacing between field centers and thus covering both sources IRAS 16293−2422A and B. However, in this study we will focus only on the molecular and continuum emission arising from IRAS 16293−2422B. The primary beam of ALMA at 690 GHz has a FWHM of $\sim$ 8 arcsec.

The ALMA digital correlator was configured in 4 spectral

[1] Centro de Radioastronomía y Astrofísica, UNAM, Apdo. Postal 3-72 (Xangari), 58089 Morelia, Michoacán, México
[2] Max-Planck-Institut für Radioastronomie, Auf dem Hügel 69, 53121, Bonn, Germany
[3] Astronomy Department, Faculty of Science, King Abdulaziz University, P.O. Box 80203, Jeddah 21589, Saudi Arabia
[4] Academia Sinica Institute of Astronomy and Astrophysics, P.O. Box 23-141, Taipei 10617, Taiwan

TABLE 1
OBSERVATIONAL AND PHYSICAL PARAMETERS OF THE SUBMILLIMETER LINES

Lines	Rest frequency[a] [GHz]	E_{lower} [K]	Range of Velocities [km s^{-1}]	Linewidth [km s^{-1}]	LSR Velocity[b] [km s^{-1}]	Line Peak flux Jy Beam^{-1}
$H^{13}CN$ [J= 8−7] $\nu = 0$	690.55207	80.6	−1,+7	4.0	−3.0	1.00
$HC^{15}N$ [J= 8−7] $\nu = 0$	688.27379	80.3	−1,+7	3.8	−3.0	1.00
CH_3OH [9(3, 6)- 8(2, 7)] $\nu_t = 0$	687.22456	84.3	−1,+7	3.8	−3.0	1.02

[a]The rest frequencies were obtained from the Splatalogue: http://splatalogue.net

windows of 1875 MHz and 3840 channels each. This provides a channel width of 0.488 MHz (~ 0.2 km s^{-1}), but the spectral resolution is a factor of two lower (0.4 km/s) due to online Hanning smoothing.

Observations of Juno provided the absolute scale for the flux density calibration while observations of the quasars J1625−254 and NRAO530 (with flux densities of 0.4 and 0.6 Jy, respectively) provided the gain phase calibration. The quasars 3C279 and J1924-292 were used for the bandpass calibration.

The data were calibrated, imaged, and analyzed using the Common Astronomy Software Applications (CASA). To analyze the data, we also used the KARMA software (Gooch 1996). The resulting r.m.s. noise for the line images was about 50 mJy beam^{-1} in a velocity width of 0.4 km s^{-1} and 20 mJy beam^{-1} for the continuum emission at an angular resolution of $0\farcs31 \times 0\farcs18$ with a P.A. = −69.3°. We used a robust parameter of 0.5 in the CLEAN task. The spectra and the physical parameters of the observed lines are shown in Figure 1 and Table 1, respectively. Many more spectral lines from different molecular species were found across the entire spectral bandwidth, however, this study will concentrate on the analysis of the continuum emission and the lines presented in Table 1 that are associated with IRAS 16293−2422B. These selected lines show a good contrast between the absorption and emission features as compared with the rest. We give the line peak emission of every line in Table 1.

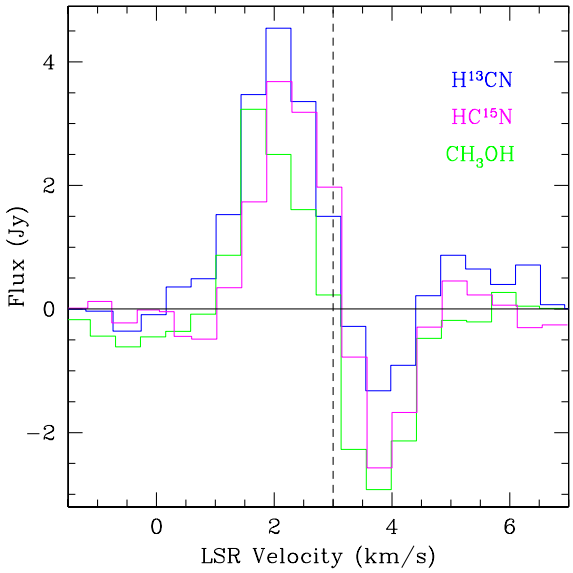

FIG. 1.— $H^{13}CN$ (blue), $HC^{15}N$ (magenta), and CH_3OH (green) summed spectra from IRAS 16293−2422B. The black dashed line marks the systemic LSR velocity of IRAS 16293−2422B (V_{LSR} ~ 3 km s^{-1}).

3. RESULTS AND DISCUSSION

3.1. *0.45 mm continuum emission*

In Figure 2, we show color and contour maps of the line and continuum emission as mapped by ALMA from IRAS 16293−2422B at these wavelengths. In this Figure, we have overlaid the resulting continuum map with the integrated intensity (moment zero) maps of the spectral molecular lines. It is clearly observed in all lines, that the molecular emission surrounds the continuum emission and has a strong central depression or "hole" in the middle.

The peak of the continuum shows a small offset to the west with respect to the central position of the "hole". This small deviation might be explained by opacity effects of the dust emission at these wavelengths. However, this shift effect is also observed at longer wavelengths by Rodríguez et al. (2005).

The dust compact source has a deconvolved size of about 400 ± 55 *milli-arcseconds* or a spatial size of 50 AU at the distance of IRAS 16293−2422. This size is quite large (a factor of about six) compared to that found at 7 mm by Rodríguez et al. (2005). This difference in apparent angular sizes is most probably the result of the increasing optical depth with frequency of the dust. Moreover, inside of the 50 AU diameter, the source B does not show any more inner structure even when our beam size is about half of the source's size at these wavelengths. This suggests that we are seeing very optically thick dust emission at these wavelengths.

The flux density of IRAS 16293−2422B at these wavelengths is 12.5 ± 0.5 Jy and has a peak flux of 3.2 ± 0.2 Jy Beam^{-1}. Using the full Planck equation, we can obtain the brightness temperature:

$$T_b = \frac{h\nu}{k \ln\left(\frac{2h\nu^3\Omega}{S_\nu c^2} + 1\right)},$$

where c is the speed of light, S_ν is the flux density, ν is the frequency, k is Boltzmann constant, and Ω is the solid angle. Following this relation, and using a Gaussian beam, we estimated a brigthness temperature at these wavelengths for IRAS16293−2422B of 160 K.

With these flux values one can estimate a lower limit for the mass of the disk. Assuming that the dust is optically thin and isothermal, the dust mass (M_d) will be directly proportional to the flux density (S_ν) as:

$$M_d = \frac{d^2 S_\nu}{\kappa_\nu B_\nu(T_d)},$$

where the d is the distance to the object, κ_ν the dust mass opacity, and $B_\nu(T_d)$ the Planck function for the dust temperature

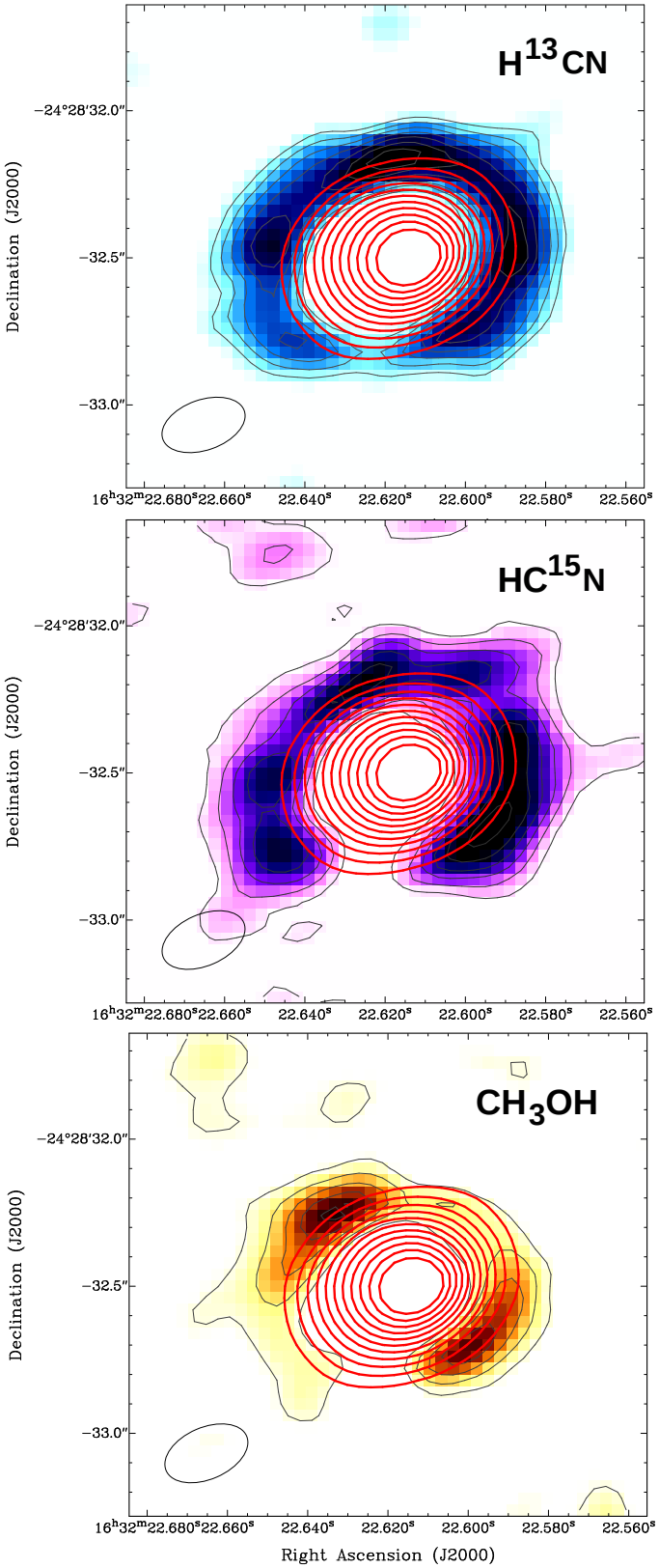

FIG. 2.— $H^{13}CN$ (blue), $HC^{15}N$ (magenta), and CH_3OH (yellow) color scale moment 0 maps from IRAS 16293−2422B overlaid in grey contours with its own line emission and in red contours with the 0.45 mm continuum emission. The red contours are from 15% to 90% with steps of 7% of the peak of the line emission; the peak of the 0.45 mm continuum emission is 3.2 Jy Beam^{-1}. For the line emission the grey contours are from 15% to 90% with steps of 5% of the peak of the integrated line emission. The synthesized beam of the continuum image is shown in the bottom left corner of each image.

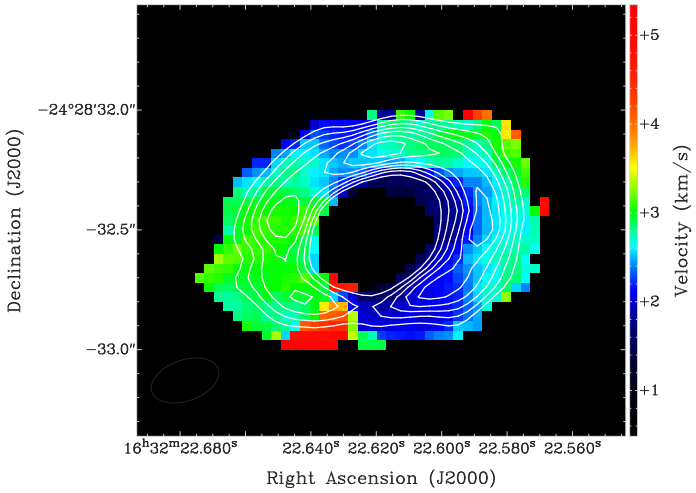

FIG. 3.— Integrated intensity of the weighted velocity (moment 1) color map of the $H^{13}CN$ emission from the source IRAS 16293−2422B overlaid in contours with the integrated intensity contour map (white). The white contours are from 15% to 90% with steps of 5% of the peak of the integrated line emission; the peak of the integrated line emission is 4.1×10^3 mJy Beam^{-1} km s^{-1}. The color-scale bar on the right indicates the LSR velocities in km s^{-1}.

T_d. Assuming a dust mass opacity (κ_ν) of 2.2 cm^2 g^{-1}, obtained extrapolating at these wavelenghts the value obtained by Ossenkopf & Henning (1994) for coagulated dust particles with no ice mantles, and at a density of 10^8 cm^{-3}. Assuming also an opacity power-law index $\beta = 0.6$ (Rodríguez et al. 2005), as well as a characteristic dust temperature (T_d) of 160 K, we estimated a lower limit for the mass for the disk of about 0.03 $M_\odot$. Please note that the level of uncertainty in the mass lower limit is a factor of five, given the range of 0.435 mm opacities in Table 1 of Ossenkopf & Henning (1994).

3.2. *Molecular line emission*

In Figure 1 and 2, as mentioned earlier, we present the integrated intensity maps (moment 0) of the molecular emission reported on this work. The spectrum from all lines were obtained averaging in an area (box) similar to the size of the molecular ring like structure (∼ 1.0″). The spectrum of all lines is found to be well centered at an LSR velocity of +3 km s^{-1}, which is approximately the systemic velocity for this source (Pineda et al. 2012; Jørgensen et al. 2011). All three lines also show marked inverse P-Cygni profiles but with that of the CH_3OH showing the more pronounced absorption feature. This is probably due to this line frequently being more optically thick. The $H^{13}CN$ and $HC^{15}N$ show line profiles very similar with the emission components being stronger compared with the CH_3OH spectra, see Figure 1. This latter line mostly shows two faint condensations surrounding the continuum source and does not present a marked ring like structure as compared with the rest of the lines.

The morphology of the line emission in general forms a well defined ring like structure around the continuum. However, the ring like structure is not completely closed, there is a small cavity towards its southeast. This cavity is probably created by the southeast monopolar outflow reported by Loinard et al. (2012). The molecular ring like structure has a diameter of 850 ± 50 *milli-arcseconds* and an inner diameter of 300 ± 50 *milli-arcseconds*, which is comparable to the deconvolved size of the 0.45 mm continuum source (about 400 *milli-arcseconds*).

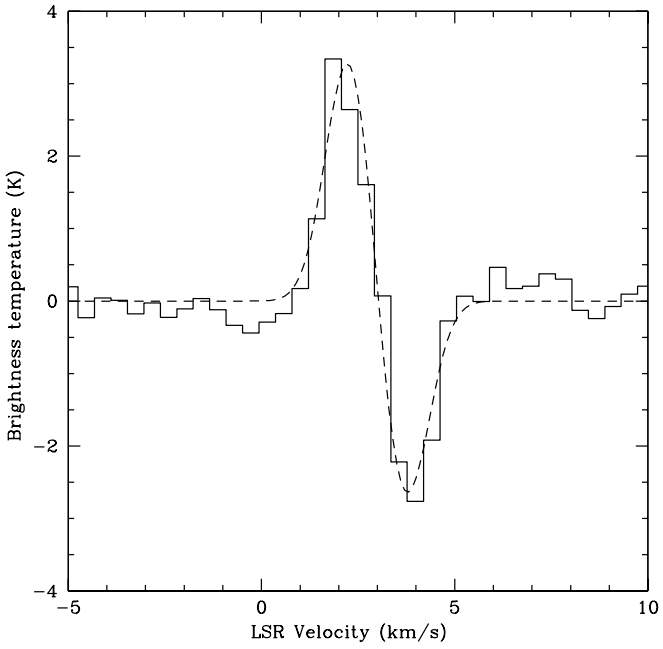

FIG. 4.— Observed (solid line) and modeled (dashed line) spectra of the CH_3OH.

In Figure 3, we show the integrated intensity of the weighted velocity (moment 1) color map of the $H^{13}CN$. This figure reveals a clear east-west velocity gradient of approximately 1.3 km s^{-1} over 60 AU. This small gradient might suggest that the orientation of the disk plane is very close to the plane of the sky. If we assume that the rotation is Keplerian and attribute it to a disk in rotation then the dynamical mass associated to this velocity gradient corresponds to only 0.1 $M_\odot$, which is indeed very small and is comparable with the dust disk mass. However, if we correct by the inclination angle dividing this mass by the $\sin\theta$ with θ say 5°, we obtain a value of 1.2 $M_\odot$, a more reasonable value for the central object and the disk associated with a solar type young star, see Correia et al. (2004). We therefore conclude that the disk plane of IRAS16293−2422B must be located almost on the plane of the sky, as already suggested by Rodríguez et al. (2005).

3.3. *Modeling*

In Figure 4, we show the result of the modeled spectra that we made in this study. We fitted the spectral profile using a modified two-layer model (Myers et al. 1996; Di Francesco et al 2001; Kristensen et al. 2012), as described by Pineda et al. (2012). This model consists of two layers of gas, front and rear, that are infalling towards the central source with an infall velocity, velocity dispersion, excitation temperature, and opacity at the center of the line of V_{in}, σ_v, T_x, and τ_0, respectively. In between the two layers there is an optically thick continuum source emitting as a blackbody of temperature T_c, and filling a fraction of the beam, Φ. The background temperature that illuminates the rear layer is taken to be the cosmic background, $T_f = 3$ K.

The brightness temperature of the optically thick continuum source is taken to be such that it matches the peak continuum flux density of the image, T_c = 160 K. The adopted filling fraction of the continuum source, Φ =0.37 is consistent with the ratio of solid angles between the region in absorption to the region in emission. From the fits of Pineda et al. (2012) to lines at lower frequencies (220 GHz) they estimate T_x = 40 K. The lines sampled by us are probably originating in gas closer to the star (see below). Assuming that the excitation temperature of the molecules decreases as the square root of the distance and that the gas sampled by Pineda et al. (2012) is 50% more distant than that sampled by us, we adopt T_x = 50 K. The fitting was minimized with a grid search, obtaining the following parameters: V_{in} = 0.7 km s^{-1}, σ_v = 0.6 km s^{-1}, and τ_0 =0.17. Finally, the systemic velocity obtained from the fit was V_{LSR} = 3.0 km s^{-1}.

Several of the parameters are quite similar to those derived by Pineda et al. (2012) from lines at 220 GHz. However, others are not and we discuss them here. First, the brightness temperature of the optically thick continuum source is 20 K in the case of Pineda et al. (2012) and 160 K in this paper. This is as expected since the optical depth of dust increases sharply with frequency. The large brightness temperature derived by us and consistent with our profile modeling implies that at 690 GHz we are observing a truly optically-thick disk since the brightness temperature is comparable with the thermodynamic temperatures expected in the inner parts of a YSO accretion disk. The optical depth used by us is about one half of that used by Pineda et al. (2012). Finally, the infall velocity and velocity dispersion required by our modeling (0.7 and 0.6 km s^{-1}, respectively) are larger than those used by Pineda et al. (about 0.5 and 0.3 km s^{-1}, respectively), implying that we may be detecting faster, more turbulent gas located closer to the central object. This is consistent with the standard picture of infall, where higher velocities occur at smaller radii. The velocities reported here are supersoinic as those reported in Pineda et al. (2012).

4. SUMMARY

In this paper, we have reported line and continuum observations obtained with ALMA at 690 GHz with a very high angular resolution (∼ 0.2 arcsec) of IRAS 16293-2422B. The main conclusions are as follows:

- The 0.45 mm continuum emission revealed a very compact object with a deconvolved angular size of about 400 *milli-arcseconds* that is associated with IRAS 16293-2422B. This size is very large compared to the one reported at 7 mm (about 8 AU) and does not show any structure inside of this diameter (or a flat structure).

- The $H^{13}CN$, $HC^{15}N$, and CH_3OH images revealed a pronounced inner depression or "hole" with a size comparable to that estimated for the submillimeter continuum.

- We suggest that the presence of this inner depression with an angular size comparable with that of the continuum source and the fact that we do not see inner structure in the continuum is produced by very optically thick dust located in the innermost parts of IRAS 16293-2422B.

- All three lines also show inverse P-Cygni profiles with infall and dispersion velocities larger than those recently reported at smaller wavelengths, suggesting that we are revealing faster, and more turbulent gas located closer to the central object.

- We report a small east-west velocity gradient in IRAS 16293-2422B observed in all lines that suggests that the disk plane of this object is likely located very close to the plane of the sky.

L.A.Z, L. L. and L. F. R. acknowledge the financial support from DGAPA, UNAM, and CONACyT, México. L. L. is indebted to the Alexander von Humboldt Stiftung for financial support. This paper makes use of the following ALMA data: ADS/JAO.ALMA#2011.0.00007.SV. ALMA is a partnership of ESO (representing its member states), NSF (USA) and NINS (Japan), together with NRC (Canada) and NSC and ASIAA (Taiwan), in cooperation with the Republic of Chile. The Joint ALMA Observatory is operated by ESO, AUI/NRAO and NAOJ.

REFERENCES

Bottinelli, S., Ceccarelli, C., Neri, R., et al. 2004, ApJ, 617, L69
Caux, E., Kahane, C., Castets, A., et al. 2011, A&A, 532, A23
Cazaux, S., Tielens, A. G. G. M., Ceccarelli, C., et al. 2003, ApJ, 593, L51
Ceccarelli, C., Castets, A., Loinard, L., Caux, E., & Tielens, A. G. G. M. 1998, A&A, 338, L43
Chandler, C. J., Brogan, C. L., Shirley, Y. L., & Loinard, L. 2005, ApJ, 632, 371
Correia, J. C., Griffin, M., & Saraceno, P. 2004, A&A, 418, 607
Di Francesco, J., Myers, P. C., Wilner, D. J., Ohashi, N., & Mardones, D. 2001, ApJ, 562, 770
Gooch, R. 1996, Astronomical Data Analysis Software and Systems V, 101, 80
Jørgensen, J. K., Bourke, T. L., Nguyen Luong, Q., & Takakuwa, S. 2011, A&A, 534, A100
Kristensen, L. E., van Dishoeck, E. F., Bergin, E. A., et al. 2012, A&A, 542, A8
Loinard, L., Torres, R. M., Mioduszewski, A. J., & Rodríguez, L. F. 2008, ApJ, 675, L29
Loinard, L., Zapata, L. A., Rodríguez, L. F., et al. 2012, MNRAS, L35
Myers, P. C., Mardones, D., Tafalla, M., Williams, J. P., & Wilner, D. J. 1996, ApJ, 465, L133
Ossenkopf, V., & Henning, T. 1994, A&A, 291, 943
Pineda, J. E., Maury, A. J., Fuller, G. A., et al. 2012, A&A, 544, L7
Rodríguez, L. F., Loinard, L., D'Alessio, P., Wilner, D. J., & Ho, P. T. P. 2005, ApJ, 621, L133
Yeh, S. C. C., Hirano, N., Bourke, T. L., et al. 2008, ApJ, 675, 454